Thymic Development of $CD4^+25^{hi}$ $Foxp3^+$ T-Regulatory Cells Echoes their Suppressogenic Capacity in Periphery

Cristina Nazarov-Stoica[1], Jacqueline Surls[1], Margaret Kehl[1], Constantin Bona[2], Sofia Casares[1,3] and Teodor-D. Brumeanu*[,1]

[1]*Department of Medicine, Division of Immunology, Uniformed Services University of Health Sciences, Bethesda, MD 20814, USA;* [2]*Department of Microbiology, Mount Sinai School of Medicine, New York, NY 10029, USA;* [3]*Naval Medical Research Center, Infectious Diseases Directorate, Silver Spring, MD 20910, USA*

Abstract: The $CD4^+25^{hi}Foxp3^+$ T regulatory (T-reg) cells are naturally-born in thymus and they are critical for maintaining the tolerance to self and non-self antigens. Foxp3 is the master-regulatory gene of development and function of this cell subset. Using two mouse strains that share the same MHC class II ($H\text{-}2^d$) haplotype, we found that Foxp3 is early expressed in the $CD3^+4^-8^-25^{+/-}44^-$ (DN3/4) double negative thymocytes. Furthermore, Foxp3 showed a differential kinetics of expression in the thymus of these two strains that were controlled through the rates of proliferation and apoptosis of T-reg precursors, but not by epigenetic alterations at the Foxp3 gene promoter. Faster T-reg proliferation and lower apoptosis were associated with higher $Foxp3^+$ thymic cell output. Also, faster proliferating T-reg precursors showed lower expression of CD3/TCR complex, leptin receptor, Bad, and Caspase3 early in the DN stage of differentiation. Despite a differential T-reg thymic output in these two mouse strains, the size of peripheral $CD4^+25^{hi}Foxp3^+$ T-reg compartment was homeostatically normalized. However, the $Foxp3^+$T-reg suppression tested in an autoimmune mouse model for diabetes was stronger in mice with a higher T-reg thymic output. These findings demonstrate a differential thymic development and suppressive capacity of $Foxp3^+$ T-reg cells in two genetic backgrounds regardless the MHC II haplotype. This raises the question of whether a differential suppressogenic capacity of the T-reg compartment may affect the susceptibility to autoimmune disorders in individuals from different ethnic groups.

Keywords: Foxp3, T regulatory cells, Thymic development, Suppressogenicity, Genetic background.

INTRODUCTION

The "professional" $CD4^+25^{hi}$ T regulatory cells (T-regs) represent a subset of T lymphocytes that differentiate in thymus as the "guardians" of immune system [1]. The T-regs control the immunoreactivity to *self* and foreign antigens, and at the same time maintain homeostasis of T-cell compartment in peripheral lymphoid organs [2-5]. Although the $CD4^+25^{hi}$ T-regs represent only 5-10% of the entire CD4 T-cell population, subtle alterations in their frequency and function associate with higher incidence of autoimmune disorders [6-12].

The $CD4^+25^{hi}$ T-reg cells express high levels of IL-2Rα chain (CD25) on the cell surface [13]. They are anergic by themselves and do not secrete IL-2, but they require IL-2 for thymic development and expansion in the peripheral lymphoid organs [14-17]. Several other surface receptors expressed on Tregs like CTLA-4, OX40 (TNFRSF4), glucocorticoid induced TNF receptor super family member (GITR), TNFR2, 4-1BB, PD1, CD103 ($\alpha E\beta 7$ integrin), Toll Like Receptors (TLR) and galectin-10, were described [18-22]. However, the Foxp3 gene encoding for the Scurfin (SFN) fork head-winged helix transcription factor is the most reliable marker for $CD4^+25^{hi}$ T-reg cells [23-25]. A mutated SFN variant is responsible for alterations in the T-reg compartment associated with X-linked autoimmune disorders in *scurfy* mice and IPEX/XLAAD syndrome (Immune Dysregulation, Polyendocrinopathy, Enteropathy, X-linked) in humans [26].

In general, patients with autoimmune diseases have a reduced number of $Foxp3^+$ T-reg cells such as those with hepatitis C virus-associated mixed cryoglobulinemia [27], autoimmune liver disease[28], juvenile idiopathic arthritis [29, 30], systemic lupus erythematosus [23, 31], Kawasaki disease [32], and psoriatic arthritis [30]. It is believed that a low frequency of circulating T-reg cells in these patients is the result of their impaired clonal expansion in the peripheral lymphoid organs [28, 33]. In contrast, no significant reduction in the peripheral, circulating T-reg cells was observed in patients with autoimmune diseases like multiple sclerosis [33, 34], autoimmune diabetes [35, 36], and spondyloarthritis [30]. Even more contrasting, patients with Sjogren syndrome showed an increased number of T-reg cells [37], and those with rheumatoid arthritis [38-42] and myasthenia gravis [38, 39] showed either reduced or unaltered number of T-reg cells. However, little is known about the function and size of T-reg compartment in autoimmune diseases in relation to Foxp3 expression and the genetic background.

This study provides evidence that two mouse strains with different genetic backgrounds (BALB/c and B10.D2) and sharing the same MHC class II haplotype ($H\text{-}2^d$) have different kinetics of $CD4^+25^{hi}Foxp3^+$ T-reg thymic development resulting in a different $Foxp3^+$ thymic output and suppres-

*Address correspondence to this author at the Department of Medicine, Division of Immunology, Uniformed Services University of Health Sciences, Bethesda, MD 20814, USA; E-mail: tbrumeanu@usuhs.edu

1876-8946/09

sogenic function in periphery. The rates of T-reg proliferation and apoptosis in thymus were found as a major mechanism leading to the differential $Foxp3^+$ thymic output in these two mouse strains. Despite a differential $Foxp3^+$ T-reg thymic output in these strains, the size of peripheral $CD4^+$ $Foxp3^+$ T-reg compartment was homeostatically normalized, although the threshold of suppressogenicity was not. Higher suppressogenicity of T-reg cells was strongly correlated with higher amount of Foxp3 protein at the single-cell level.

MATERIALS AND METHODOLOGY

Mice

One-month-old, female BALB/c and B10.D2 ($H\text{-}2^d$) mice were purchased from Jackson Laboratories. The TCR-HA and RAG2 KO, RIP-HA transgenic (Tg) mice used in the adoptive cell co-transfer experiments are currently maintained in our facilities. Mice were housed at USUHS in a pathogen-free facility according to federal and local regulations.

Cell Purification

The $CD4^+$ thymocytes and splenocytes from pools of mice (n = 4-6) were negatively sorted on mouse CD4 enrichment columns (R & D Systems, Minneapolis, MN) according to the manufacturer's protocol. A second passage of $CD4^+$ cells on mouse CD8 enrichment columns (R & D Systems) yielded negatively-sorted $CD4^-8^-$ DN thymocytes. The purity and viability of thymic populations was more than 90% as determined by FACS and trypan blue exclusion method. The $CD4^+25^+$ thymocytes and splenocytes were isolated on MS MACS paramagnetic columns (Miltenyi Biotech Inc., Auburn, CA). Briefly, the negatively-sorted $CD4^+8^-$ single positive (SP4) or $CD4^-8^-$ double negative (DN) cells were incubated with anti-CD25-PE Ab-dye conjugate for 10 min, washed, and further incubated anti-PE Ab-microbeads for 15 min. The cells were sorted on magnetic columns (Miltenyi Biotec) into a $CD25^-$ fraction (cell flow through) and a $CD25^+$ fraction (T-regs, column bound cells). In some experiments, the DN thymocytes were stained with anti-CD44 and CD25 Ab-dye conjugates and sorted by a FACSAria instrument/FACSDiva software (Becton Dickinson) into DN1-4 or $CD4^+25^{hi}$ subpopulations at 97-98% purity.

RT-PCR and Quantitative Real-Time RT-PCR

Total RNA and cDNA from $CD25^+$ and $CD25^-$ thymocytes was prepared using NucleoSpin RNA II kit (BD Biosciences Clontech, Palo Alto, CA) and Qiagen One Step RT-PCR kit (Qiagen Inc., Valencia, CA) respectively, as previously described [43]. The primers for murine Foxp3 were: (forward 5'CAGCTGCCTACAGTGCCCCTAG3', and reverse 5'CATTTGCCAGCA GTGGGTAG3' [23], Fas (forward CGCTGTTTTCCCTTGCTGCAG, reverse ACAGG TTG GTGTACCCCCAT) [44], Fas-L (forward CACTGAC CCCTCTAAAGAAGAA, reverse TTGAATACTGCCCCC AGGTA) [45]. The specific primers for Bcl-2, Bcl-X_L, Bad, Bax, and Caspase 3 were previously described [43]. Four nanograms of total RNA were used to prepare first-strand cDNA using a Qiagen One Step RT-PCR kit (Qiagen, Valencia, CA) at 35 and 40 cycles of amplification following the manufacturer's protocol. 25μL of each PCR product was then electrophoresed in 1.5% agarose gel containing ethidium bromide, and the amount of each amplicon was calculated using the Scion Image software analysis (Scion Corp., Frederick, MD) based on the integration of the percent of pixels and band intensity after normalization against the corresponding β-actin band [43]. To measure the expression level of Foxp3 by quantitative real–time RT-PCR, the RNA was extracted from various thymic populations using Total RNA Purification System (Invitrogen). Some 500 ng RNA was used to synthesize the first cDNA strand using the High Capacity cDNA Archive kit (Applied Biosystems). PCR amplification mixtures containing the Applied Biosystems Universal PCR MasterMix Buffer (25 μl), cDNA template (22.5μl), Foxp3 and 18S rRNA primers (2.5 μl), respectively. Quantitative RT-PCR measurements were performed on an ABI Prism 7700 with SDS 1.9.1 Software (Applied Biosystems). The melting-curve analysis has confirmed the specificity of PCR amplifications. The relative mRNA levels were estimated by the standard method using 18S rRNA as reference.

Cytofluorimetry

Thymocytes or splenocytes ($2x10^5$) were surface, intracellularly, or intra-nuclearly stained with various antibody-dye conjugates, their isotype controls, or with Annexin V-PE conjugate according to the manufacturer's instructions (BD PharMingen, San Diego, CA). Between 200,000 and 500,000 total cell events were acquired by a LSR II Bekton-Dikinson instrument for each cell preparation. For accurate measurements of mean fluorescence intensity (MFI) at the single-cell level, the slight difference in the cell size and signal-to-noise cell autofluorescence were compensated with WINlist analysis software 3D5.0 (Verity Software House, Topsham, ME) during the data acquisition. Measured parameters were compared under various experimental conditions using the Sigmaplot analysis software v.8 (Aldrich-Sigma). Overall data were presented for convenience as mean ± SD of pooled samples.

In Vivo Cell Cycle Division

Mice were injected intravenously (i.v.) with 1 mg of carboxyfluorescein succinimidyl ester (CFSE) in saline, and then one, four, and six days later some 1 x 10^6 gated $CD4^+CD25^{hi}$ T-reg cells isolated from the thymus and spleen were harvested. Data on cell cycle division were acquired using a LSR II instrument (BD Biosciences). The pattern and number of cell cycle divisions based on the CFSE dilution factor were analyzed with the WINlist software 3D 5.0.

Caspase 3 Activity

Some 25μg of protein extract from DN thymocytes isolated as described were incubated for 40 min in 96-well plates in 100 μl buffer (100 mM HEPES, 10% sucrose, 0.15% CHAPS, 10 mM DTT, 0.1 mg/ml ovalbumin, pH 7.4) supplemented with 1 μM of substrate (Ac-DEVD-AMC, Peptide Intern., Louisville, KY) at 37^0C. The amount of substrate released was measured in a spectrofluorimeter (excitation λ = 360 nm and emission λ = 436 nm) equipped with an XFluor analysis software (Tecan US, Durham, NC). Standard dilutions of the substrate were used in each assay to measure the absolute concentration of released AMC, and the measured fluorescence units were converted into rate of AMC cleavage per mg protein (corresponding to pmole

cleaved DEVD-AMC x min^{-1} x mg^{-1}). Values were compensated for the signal-to-noise background (spontaneous release of AMC in the absence of cell extract)

Adoptive Cell Transfers

The RAG2 KO, RIP-HA Tg mice (BALB/c x B10D2, H-2^d background) expressing the hemagglutinin protein (HA) of influenza PR8 virus in the pancreatic β-cells under the rat insulin promoter [10] were used as recipients of splenic $CD4^+25^{hi}$ $Foxp3^+$ T-reg cells (10^5 cells) isolated from BALB/c or B10.D2 mice, and/or diabetogenic HA-specific $CD4^+25^-$ Th cells (2.5 x 10^5 cells) isolated from BALB/c mice expressing the HA-TCR transgene (TCT-HA Tg) that recognizes the HA110-120 immunodominant CD4 T-cell epitope of HA of PR8 influenza virus in context of MHC class II H-2^d haplotype [46]. The TCR-HA Tg mouse expresses the TCR-HA transgene on 35-40% splenic CD4 T-cells. The i.p. infusion of diabetogenic $CD4^+25^-$ T-cells from TCR-HA Tg mice (2.5 x 10^5 cells) in RAG2 KO, RIP-HA Tg mice induces a rampant hyperglycemia followed by death within 12 to 14 days. The T-reg cells were infused i.p. 7 days prior infusion of diabetogenic TCR-HA T-cells.

Diabetes Monitoring

Glycemia in the RAG2 KO, RIP-HA Tg recipients of T-regs and diabetogenic T-cells was monitored by-weekly starting 3 days post transfer of diabetogenic T-cells by using Accu-Check Advantage glucose strips (Boehringer Manheim, Indianopolis, IN). Mice were considered diabetic when glycemia was two-times consecutively over 200 mg/dl. One week after the transfer of diabetogenic T-cells, 2 pancreases were collected from each group of mice and analyzed histochemically for the presence of lymphocyte infiltration of the pancreatic β-islets using hematoxilin-eosin (HE) staining of paraffin-embedded pancreatic sections. Survival in the RAG2 KO, RIP-HA Tg recipients was also monitored on a daily basis.

DNA Methylation Assay

Genomic DNA was isolated from purified thymocytes of 1 month-old mice BALB/c and B10.D2 mice using the DNeasy tissue kit (Qiagen, Valencia, California, United States) and following the supplier's recommendations. Sodium bisulphite treatment of genomic DNA was performed as previously described [47] with minor modifications aimed at deamination of unmethylated cytosines to uracil, whereas the methylated cytosines remained unchanged. In a subsequent PCR amplification, uracils were replicated as thymidines. Thus, detection of a ''C-element'' in sequencing reactions indicated methylation of the genomic DNA. Detection of a ''T-element'' at the same site indicated instead the absence of a methyl modification of the genomic cytosine. PCRs were performed in a final volume of 25 µl containing 13 µl PCR buffer, 1-U Taq DNA polymerase (Qiagen), 200 lM dNTPs, 12.5 pmol each of the forward and reverse primers, and 7 ng of bisulphate treated genomic DNA. The amplification conditions were 95° C for 15 min and 40 cycles at 95° C for 1 min, 55° C for 45 sec, and 72° C for 1 min with a final extension step of 10 min at 72° C. PCR products were purified using Qiagen MinElute gel extraction kit, sequenced in both directions applying the PCR primers and the ABI Big Dye Terminator v1.1 cycle sequencing chemistry (Applied Biosystems, Foster City, California, United States), and measured by capillary electrophoresis on an ABI 3100 genetic analyzer. For each sample, both the PCR amplification and sequencing analysis were repeated twice. The following primers specific for the murine Foxp3 gene promoter (5' to 3' direction) were used for both PCR amplification of bisulphite converted genomic DNA and sequence reactions: Amp 1 (forward: AGGAAGAGAAGGGGGTAGATA; reverse: AAACTAACATTCCAAAACCAAC), Amp 2 (forward: ATTTGAATTGGATATG GTTTGT; reverse: AACCTTA AACCCCTCTAACATC).

Statistic Analysis

Significance of survival of RAG2 KO, RIP-HA Tg recipients of T-regs and diabetogenic T-cells was determined along with that of control groups by Kaplan-Meier test. The significance of individual differences in MFI measured by FACS, and percentage of cell populations in different groups of mice analyzed by FACS was determined by the Student's *t*-test.

RESULTS

The DN Stage of Thymic Differentiation is an Early Time-Point of Foxp3 Expression

Studies on the murine thymic development showed that at day 12 of gestation the bone marrow-derived T cell precursors migrate to the thymic cortico-medullary junction as triple negative $CD3^-4^-8^-$ cells [48, 49]. They then differentiate into double negative DN1($CD4^-8^-44^+25^-$) and DN2 ($CD4^-8^-44^+25^+$) stages and enter the subcapsular cortex to differentiate into DN3 ($CD4^-8^-44^-25^+$) cells and DN4 ($CD4^-8^-44^-25^-$) cells. The DN4 cells migrate further to the cortex to proliferate and differentiate into double positive DP ($CD4^+8^+$) cells expressing a mature α/β heterodimer TCR on the surface. The majority of DP cells undergo a negative selection by apoptosis-induced cell death leading to elimination of *self*-reactive precursors. Few DP cells undergo positive selection to generate single positive (SP) T cells ($CD4^+8^-$ or $CD4^-8^+$) with low or no specificity for *self*-antigens [50] that migrate to periphery.

Foxp3 transcripts were previously detected by RT-PCR in $CD4^+8^+$ double positive (DP) and $CD4^+8^-$ single positive (SP4) thymocytes of BALB/c mice [23]. Herein, we have analyzed the kinetics of Foxp3 mRNA and protein in T-reg precursors from BALB/c and B10.D2 mice during different stages of thymic differentiation. The $Foxp3^+$ thymocytes are thereafter referred as T-reg precursors.

The B10.D2 inbred mouse strain on a C57BL/6 background shares the same MHC class II haplotype (H-2^d) with the BALB/c mouse. In both strains, Foxp3 mRNA was barely detected by RT-PCR in DN thymocytes (Fig. **1A**), but they were clearly detected by real-time RT-PCR (Fig. **1B**). The level of Foxp3 mRNA in DN thymocytes from B10.D2 was higher than that in BALB/c mice and this was paralleled by an increased Foxp3 intranuclear expression as measured by single-cell level FACS (Fig. **1C**). We next measured the kinetics of Foxp3 mRNA expression among the FACS-sorted DN1, DN2, DN3 and DN4 thymic populations (Fig. **1D**), and by quantitative real-time RT-PCR. The Foxp3 transcripts were detected in the DN3 and DN4 thymocytes in

both strains, but not in the DN1 and DN2 thymocytes (Fig. **1E**).

A differential Foxp3 expression in the BALB/c and B10.D2 thymocytes raised the question of whether genetic or post-translational events may control the Foxp3 expression in thymus. The 1st and 2nd amplicon of Foxp3 promoter located upstream of exon 1 is the most susceptible region for DNA methylation [51]. Our bisulfite-mediated DNA methylation assay in the $CD4^{+}25^{hi}$ T-reg precursors ruled out the possibility of a differential DNA methylation in the Foxp3 gene promoter in T-reg precursors as a possible mechanism responsible for variations in the thymic expression of Foxp3 gene in BALB/c and B10.D2 thymocytes. That is because this region showed 100% homology in T-reg precursors, and an equal number of CpG potential sites of methylation (15 sites) in the 1st and 2nd amplicon of Foxp3 promoter in both strains (Fig. **2**).

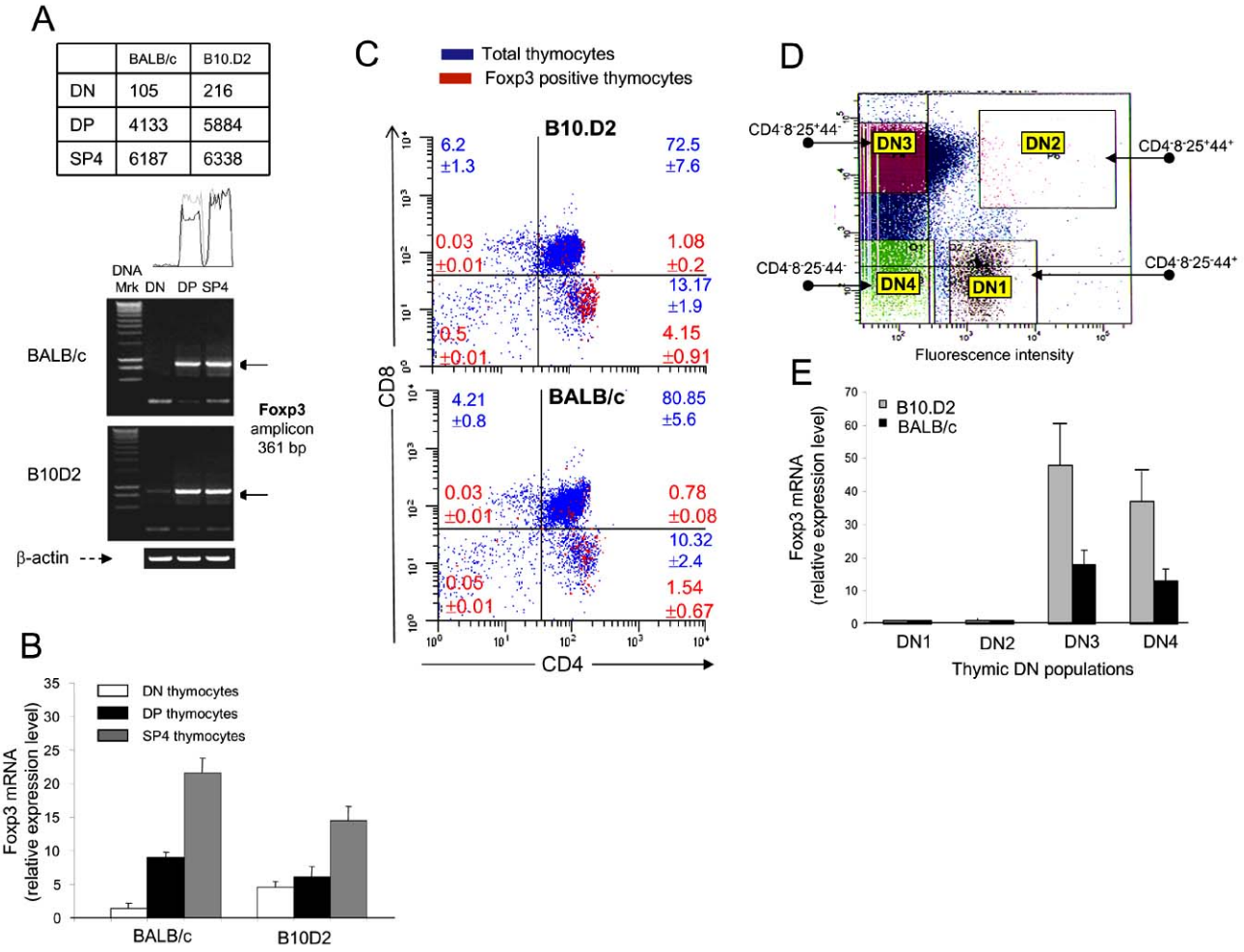

Fig. (1). Kinetics of Foxp3 expression in T-reg precursors from BALB/c (H-2^{d}) and B10.D2 (H-2^{d}) mice. (**A**) $CD4^{-}8^{-}$ (DN), $CD4^{+}8^{+}$ (DP), and $CD4^{+}8^{-}$ (SP4) thymocytes analyzed by RT-PCR for Foxp3 mRNA expression. Shown are the Foxp3 transcripts at 40 cycles of PCR amplification for a representative BALB/c and B10.D2 mouse. Similar results were obtained in other five mice. Foxp3 transcripts could not be detected in DN thymocytes at 35 cycles of PCR amplification (not shown). Upper panel indicates the absolute values of Foxp3 amplicon in each thymic population from the two strains as measured by ScionImage analysis software. (**B**) Quantitative measurements of Foxp3 transcript in thymic populations as determined by quantitative RT-PCR. The relative expression level of Foxp3 mRNA (Y-axis) measured in DN, DP, and SP4 thymocytes from BALB/c and B10.D2 mice was calculated in relation to the base level of Foxp3 mRNA as found in BALB/c DN thymocytes. Shown are the mean values ± SD from six individual mice in each group. (**C**) Distribution of $Foxp3^{+}$T-reg precursors in thymus. Thymocytes from three individual BALB/c and B10.D2 mice were cell surface stained with CD4-PE-Cy7 and CD8-PerCP, and intranuclear with Foxp3-PE Ab-conjugates. Overlapped forward scatters in each quadrant indicate the percent ±SD of total DN, DP, SP4 and SP8 thymocytes (blue color) *vs* Foxp3-expressing thymocytes (red color) within the DN, DP, SP4 and SP8 thymic populations. The signal-to-noise background fluorescence of a rat IgG isotype PE conjugate control for Foxp3 was subtracted. Some 850,000 total cell events were acquired by a LSR II instrument and analyzed by WINList software. (**D**) FACS-sorting of DN1-4 thymic subpopulations. Gated DN thymocytes from BALB/c or B10.D2 mice were stained with CD4 and CD8 PerCP-Ab conjugates, and sorted based on CD44-FITC and CD25-APC Ab staining. (**E**) Measurements of Foxp3 transcript in DN1-4 thymocytes by quantitative real-time PCR. Shown are the mean values ± SD for Foxp3 mRNA as extracted from FACS-sorted DN1-4 thymocytes of three BALB/c and B10.D2 mice.

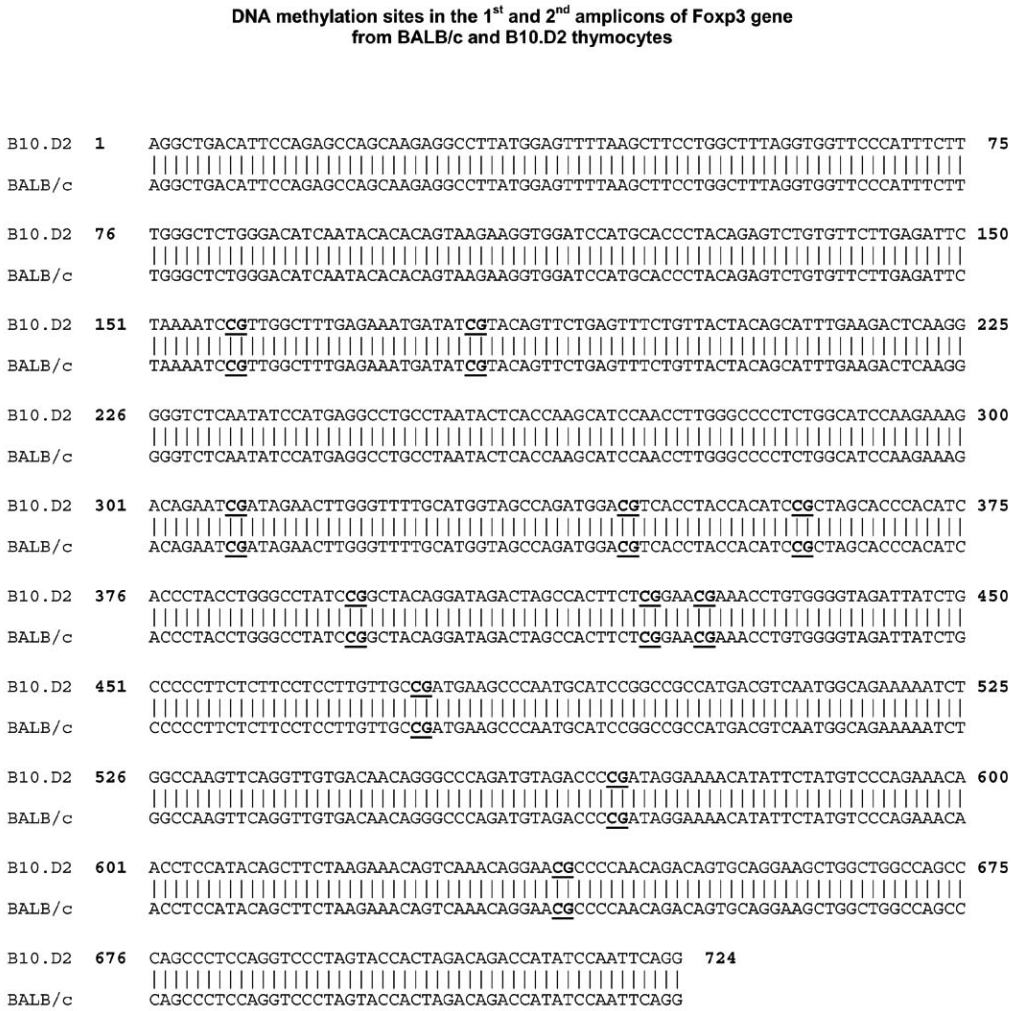

Fig. (2). Frequency of CpG motifs in the 1st and 2nd amplicon of Foxp3 gene promoter in T-reg precursors from BALB/c and B10.D2 T-reg precursors. Individual CpG motifs are marked as bold/underlined base pairs, and the alignment of BALB/c and B10D2 genomic sequences corresponding to the overlapping amplicons #1 and #2 in the Foxp3 gene promoter in T-reg precursors are shown.

These results demonstrated for the first time that the earliest time-point of Foxp3 expression in thymus is the DN3/4 stage of differentiation. A differential Foxp3 expression and Foxp3 thymic output in BALB/c and B10.D2 mice sharing the same H-2^d (MHC class II) haplotype suggests that other genes that MHC class II genes may control the Foxp3$^+$ thymic output.

The T-Reg Precursors have Higher Proliferation Rate in the B10.D2 Mice than in BALB/C Mice

Since the BALB/c and B10.D2 mice showed a differential Foxp3 thymic output, we first compared the *in vivo* proliferation rates of T-reg precursors during the thymic differentiation by measuring the CFSE dilution factor in relation to the number of cell cycle divisions. The BALB/c and B10.D2 thymocytes uptake equal amounts of CFSE per cell *in vivo* as determined 30 min post injection (Fig. **3A**, two upper panels, grey peaks). Since the Foxp3 intranuclear staining quenches the CFSE fluorescence, herein we identified T-reg precursors based on their CD25^{hi} expression, a reliable biomarker of CD4$^+$ Foxp3$^+$ T-regs. More than 95% of CD4$^+$Foxp3$^+$ cells express the CD25^{high} marker. The BALB/c DP (CD25^{hi}) and SP4 (CD25^{hi}) T-reg precursors exhibited a lower rate of thymic proliferation (4-5 cycles of division on day 4, and 5-6 cycles of division on day 6 post-CFSE-labeling) as compared with their B10.D2 counterparts (5-6 cycles on day 4 ,and 7-8 cycles on day 6 post-CFSE-labeling) (Fig. **3A**, two upper panels). This clearly indicated a differential rate of proliferation of BALB/c and B10.D2 T-reg precursors during their thymic development.

Leptin is a hormone that binds the Obese Receptor (ObR) and regulates cholesterol synthesis. Since we have previously found a differential partitioning of plasma membrane lipid rafts on the thymic T-cell precursors [52], and the leptin hormone was shown to negatively regulate the proliferation of human T-cells [21], we thought to investigate whether the levels of serum leptin and the expression level its receptor (ObR) on T-reg precursors may influence the rate of T-reg proliferation in the thymus of these two mouse strains. The serum leptin concentration measured by ELISA was similar in B10.D2 mice (4.8 ± 0.6 μg/ml) and BALB/c mice (4.5 ± 0.4 μg/ml) (n = 7 mice per group), which ruled out the possibility that the proliferation rates of T-reg precursors is

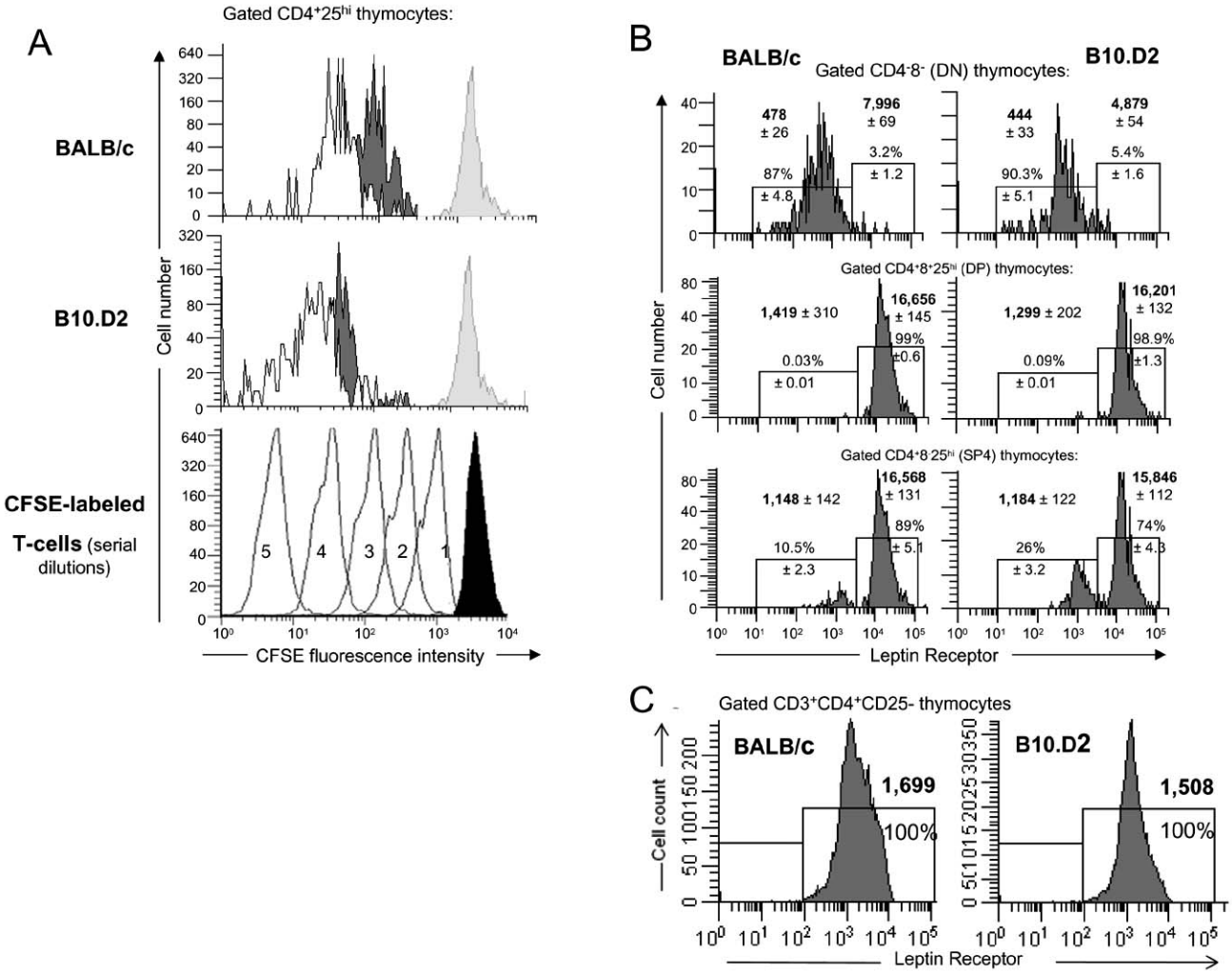

Fig. (3). ***In vivo*** **thymic proliferation of T-reg precursors from BALB/c and B10.D2 mice.** The BALB/c and B10.D2 mice (n = 5 per group) were injected i.p. with CFSE, and four and six days later the thymocytes were over stained with CD4-PE-Cy7 and CD25-APC Ab-conjugates. The number of cell cycle divisions in FACS-gated $CD4^+25^{hi}$ thymocytes was established based on the dilution factor for CFSE fluorescence. (**A**) Cell cycle divisions of FACS-gated $CD4^+25^{hi}$ thymocytes in a representative BALB/c and B10.D2 mouse. Empty histograms represent day 6, and dark histograms represent day 4 post CFSE injection. Lower panel shows the CFSE fluorescence after five serial, two-fold dilutions *in vitro* (empty plots, using ex-vivo thymocytes from a BALB/c mouse) as compared with the uptake of CFSE by thymocytes *in vivo* some 30 min after CFSE injection (grey color plots). Same MFI values were obtained when B10.D2 thymocytes were used in the two-fold dilutions *experiments* (data not shown). The two-fold serial dilutions refer to the fluorescence intensity (MFI) for each *in vitro* dilution factor (1: 1 through 1:5 of CFSE) of the CFSE-labeled thymocytes. (**B**) Partitioning of ObR on thymic T-reg precursors from BALB/c and B10.D2 mice as determined by FACS using ObR-FITC Ab-conjugate (BD PharMingen). Shown are the MFI ± SD values (bold), and percent of mean ± SD of the DN, DP $CD25^{hi}$, and SP4 $CD25^{hi}$ thymocytes from individual mice (n = 5 per group). (**C**) Partitioning of ObR on conventional CD4 T-cell thymic precursors from the spleen of BALB/c and B10.D2 mice as determined by FACS using ObR-FITC Ab-conjugate (BD PharMingen). Shown are the MFI ± SD values (bold), and percent of ObR^{low} and ObR^{high} populations within gated $CD3^+CD4^+CD25^-$ thymocytes from a pool of five mice in each group.

controlled by leptin. However, FACS analysis at the single-cell level in the $Foxp3^+$ thymic populations revealed several findings. First, we found a lower ObR expression on DN thymocytes than on DP $CD25^{hi}$ T-reg precursors in both mouse strains (Fig. **3B**). Secondly, two distinct subpopulations of low and high ObR expression (ObR^{lo} and ObR^{hi}) were detected in the SP4 $CD25^{hi}$ T-reg precursors in both mouse strains (Fig. **3B**). The B10D2 mice expressed a larger population of SP4 $CD25^{hi}$ ObR^{lo} T-reg precursors than their BALB/c counterparts, suggesting that the ObR cell density affects the thymic proliferation of T-reg precursors. Indeed, analysis of the *in vivo* cell cycle divisions of ObR^{lo} and ObR^{hi} populations of T-reg precursors showed an inverse correlation with the rate of proliferation (Fig. **4A**). The ObR^{lo} population proliferated quite faster than the ObR^{hi} population. This was consistent in two different experiments and confirmed by the Cdk4 expression level, a cyclin that is actively involved in transition of T-cells from G_0 to S_1 phase of division. The Cdk4 expression was higher in B10D2 T-reg precursors (having a larger population of fast-dividing ObR^{lo}

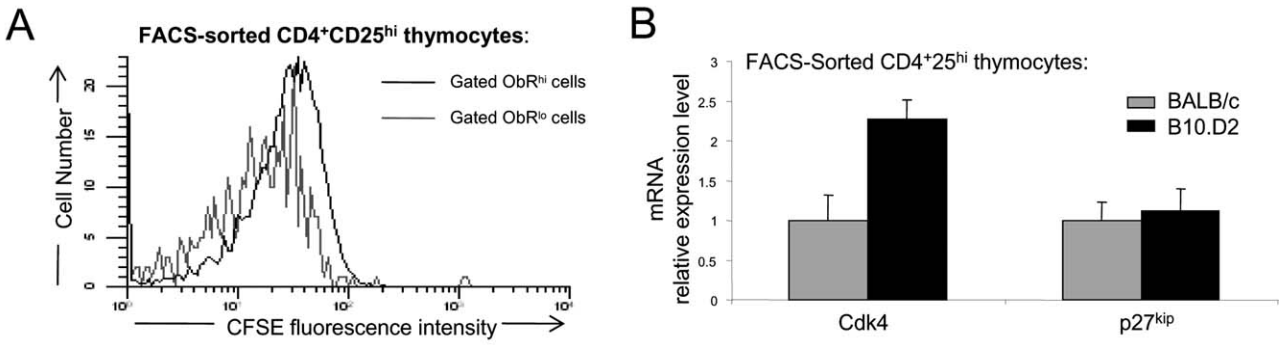

Fig. (4). ***In vivo*** **thymic proliferation of ObR^{hi} and ObR^{lo} T-reg precursors from BALB/c and B10.D mice.**

(**A**) *In vivo* cell cycle progression of ObR^{hi} and ObR^{lo} T-reg precursors. Cells from four individual CFSE-labeled BALB/c and B10.D2 mice were stained 6 days post-CFSE labeling with CD4-PE-Cy7, CD25-APC, and ObR-FITC Ab-conjugates, and the CFSE fluorescence was measured by FACS in gated (SP4) CD3$^+$CD4$^+$CD25$^-$ thymocytes. Shown are the cell cycle progression of the CD4$^+$25^{hi}ObR^{lo} and CD4$^+$25^{hi}ObR^{hi} T-reg precursors from a representative BALB/c mouse out of 3 different mice, for which the standard deviation was within a +/- 4.5 MFI range. (**B**) Cdk4 and p27^{kip} mRNA expression in FACS-sorted SP4 CD25^{hi} thymocytes from BALB/c and B10.D2 mice as measured by real-time RT-PCR (specific primers, Applied Biosystems, Foster City, CA). The relative mRNA expression (Y-axis) refers to the mRNA fold increase as compared with an arbitrarily considered "1-fold increase" as the lowest level observed in BALB/c mice).

T-reg precursors) than in BALB/c T-reg precursors (having a larger population of slow-dividing ObR^{hi} T-reg precursors) (Fig. **4B**). There was no difference in the p27^{kip} mRNA expression (a major Cdk4 inhibitor) between the BALB/c and B10.D2 T-reg precursors (Fig. **4B**). Accordingly, the ObR^{lo} T-reg precursors are faster dividers than the ObR^{hi} T-reg precursors, which implies that ObR exerts a negative regulatory effect on the proliferation of T-reg precursors.

Interesting enough, the overall ObR expression on T-reg thymic precursors was significantly higher (1 log) than that on the conventional (CD4$^+$25$^-$) T-cell thymic precursors (Figs. **3B** *vs.* **3C**) in both strains. Thus, besides a negative regulatory effect on the thymic proliferation of T-reg precursors, the ObR^{hi} expression appears to be a new biomarker for Foxp3$^+$ T-reg cells.

The T-Reg Precursors Die at Different Rates in the Thymus of BALB/C and B10.D2 Mice

Thymic apoptosis is a major mechanism for negative selection that aims at maintaining T-cell central tolerance to *self*-antigens. Thus, we investigated whether a lower T-reg thymic output in BALB/c mice than in B10.D2 mice may also account for a higher rate of elimination by apoptosis. T-reg precursors in BALB/c mice showed a higher degree of apoptosis than their counterparts from B10.D2 mice at all stages of differentiation as measured by Annexin V binding (Fig. **5**).

The sensitivity of T-cells to undergo apoptosis (negative selection) is controlled at the intra-cellular level by several pro- or anti-apoptotic proteins. Signaling through Fas receptor up-regulates expression of Bad, Bax, and Caspase-3, and leads to apoptosis. On the other hand, their cell survival relies on activation of Bcl-2 and Bcl-XL. We thus measured the basal expression of these pro- and anti-apoptotic proteins in (CD4$^+$25^{high}) T-reg precursors in comparison with the (CD4$^+$25$^-$) conventional T-cell precursors isolated from the thymus of B10.D2 and BALB/c mice. The BALB/c SP4 T-reg precursors expressed higher basal levels of Bad and Caspase-3 than their B10.D2 counterparts (Table **1**). There were no differences in the expression levels of Bcl-2 and Bcl-XL between the two strains. Interestingly, the difference in the basal level of Bad and Caspase 3 expression between the two strains was only observed in the T-reg precursors, but not in the conventional T-cell precursors. These results imply first, that the apoptotic program in T-reg precursors is differentially regulated than in conventional T-cell precursors. Secondly, in addition to the differential rates of proliferation in T-reg precursors in these two strains, a differential rate of apoptosis may have been also affected the Foxp3 thymic output.

The extent of thymic selection of T-cell precursors depends greatly on the strength of CD3/TCR interaction with MHC-peptide complexes presented by the thymic stromal cells. Can the cell density of CD3/TCR complex and CD28 co-stimulatory receptor influence the threshold of activation-induced cell death in T-reg precursors? Measuring the CD3 and CD28 mean fluorescence intensity (MFI) on T-reg precursors from BALB/c and B10.D2 mice by single-cell FACS analysis showed that the expression of CD3ε chain (but not of CD28 receptor) on the DN and DP T-reg precursors was higher in BALB/c mice than in B10.D2 mice (Fig. **6A**). To determine whether the strength of CD3 signaling is associated with the sensitivity to apoptosis in the T-reg precursors from BALB/c and B10.D2 mice, cells were stimulated with various doses of CD3 Abs, a surrogate of TCR stimulation, and then measured for the extend of Annexin V binding. The DN, DP and SP4 T-reg precursors from BALB/c mice were more sensitive to CD3-induced apoptosis than their B10.D2 counterparts (Fig. **6B**). Similar experiments using CD28 Abs indicated a lack of correlation between the strength of CD28 signaling and sensitivity to apoptosis of T-reg precursors in both strains (data not shown). These results demonstrated that the strength of CD3 signaling can affect the sensitivity of T-reg precursors to apoptosis. Thus, higher expression of CD3/TCR per cell in the BALB/c DN and DP T-reg precursors than in B10.D2 T-reg precursors may translate into a higher rate of elimination of T-reg precursors in BALB/c mice. This, in addition to a lower proliferation rate may contribute to a lower Foxp3 thymic output in BALB/c mice.

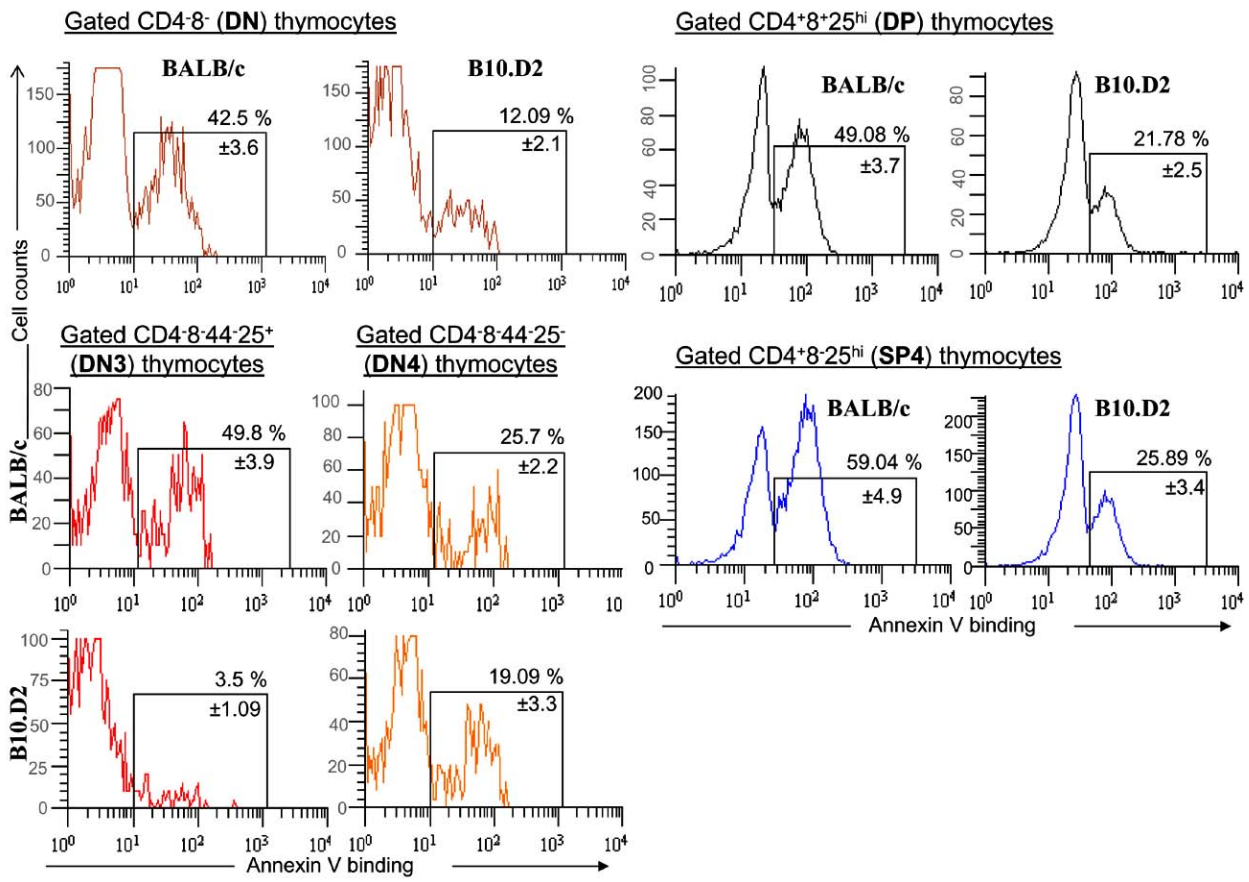

Fig. (5). ***In vivo*** **thymic cell death of T-reg precursors from BALB/c and B10.D2 mice.** Thymocytes from BALB/c and B10.D2 mice (n = 5 per group) were stained with CD4-FITC, CD8-APC, CD25-PerCP-Cy5.5 Ab-conjugates, and Annexin V-PE conjugate. For measuring Annexin V in the DN3 and DN4 populations of T-reg precursors, thymocytes were stained with CD4-PerCP, CD8-PerCP, CD44-FITC, CD25-APC Ab-conjugates and Annexin V-PE conjugate. Shown are the percent ±SD values of FACS-gated thymic populations of T-reg precursors binding the Annexin V from three different experiments.

Table 1. Expression of Pro- And Anti-Apoptotic Proteins in T-Reg Precursors *vs*. Conventional T-Cell Precursors from BALB/C and B10.D2 Mice

Apoptotic Markers		BALB/c		B10.D2	
		Thymocyte Subset			
		$CD4^+25^-$	$CD4^+25^{hi}$	$CD4^+25^-$	$CD4^+25^{hi}$
Bcl-2	mRNA*	3,112	2,815	3,260	2,964
	Protein**	152	124	148	136
	Activity***	-	-	-	-
$Bcl\text{-}X_L$	mRNA	1,420	1,114	1,408	1,203
	Protein	161	86	141	87
	Activity	-	-	-	-
Bad	mRNA	1,405	**4,118**	1,207	1,340
	Protein	67	**281**	66	99
	Activity	-	-	-	-
Bax	mRNA	731	864	750	916
	Protein	58	72	72	78
	Activity	-	-	-	-
Caspase3	mRNA	3,311	**13,211**	3,018	5,794
	Protein	-	-	-	-
	Activity	2.9	**6.3**	2.7	0.9

(Table 1). Contd…..

Apoptotic Markers		BALB/c		B10.D2	
		Thymocyte Subset			
		$CD4^+25^-$	$CD4^+25^{hi}$	$CD4^+25^-$	$CD4^+25^{hi}$
Fas	mRNA	4,812	5,105	4,601	4,818
	Protein	287	302	276	281
	Activity	-	-	-	-
FasL	mRNA	2,013	2,008	2,020	2,051
	Protein	105	114	112	109
	Activity	-	-	-	-

The mRNA and protein expression levels of anti-apoptotic and pro-apoptotic proteins in $CD4^+CD25^+$ and $CD4^+CD25^-$ thymocytes from a pool of BALB/c or B10.D2 mice (n = 5) were sorted on MACS immunobeads and analyzed for Bcl-2, Bcl-X_L, Bad, Bax, Caspase 3, Fas, and FasL by RT-PCR, and by FACS intra-cellular staining. The enzymatic activity of Caspase 3 (pmole cleaved DEVD-AMC x min^{-1} x mg^{-1}) was determined by ELISA as described. Values for the RT-PCR amplicons at 40 cycles of amplification represent the relative mRNA expression level. The protein expression levels refer to the mean fluorescence intensity (MFI) determined by FACS intracellular staining upon subtracting the signal-to-noise background of the corresponding isotype control antibody-dye conjugates. Bolded/underlined values indicate the differential expression and activity of Bad and Caspase 3.
*mRNA expression level as measured by RT-PCR and quantified by Scion Image Analysis Software.
**Protein expression level as determined by MFI in FACS at the single-cell level.
***Enzymatic activity as determined by ELISA.

A

Thymocytes	*CD3ε*		*CD28*	
	B10.D2	BALB/c	B10.D2	BALB/c
	Mean Fluorescence Intensity (MFI)			
$CD4^-8^-$ (**DN**)	67.60 ± 5.6	141.75 ±19.4	13.58 ± 2.3	12.41 ± 1.8
$CD4^+8^+25^{hi}$ (**DP**)	118.85 ± 15.5	472.87 ± 23.1	10.40 ± 3.1	10.19 ± 2.0
$CD4^+8^-25^{hi}$ (**SP4**)	296.65 ±14.7	309.84 ± 12.4	36.65 ± 3.7	30.41 ± 5.1

B

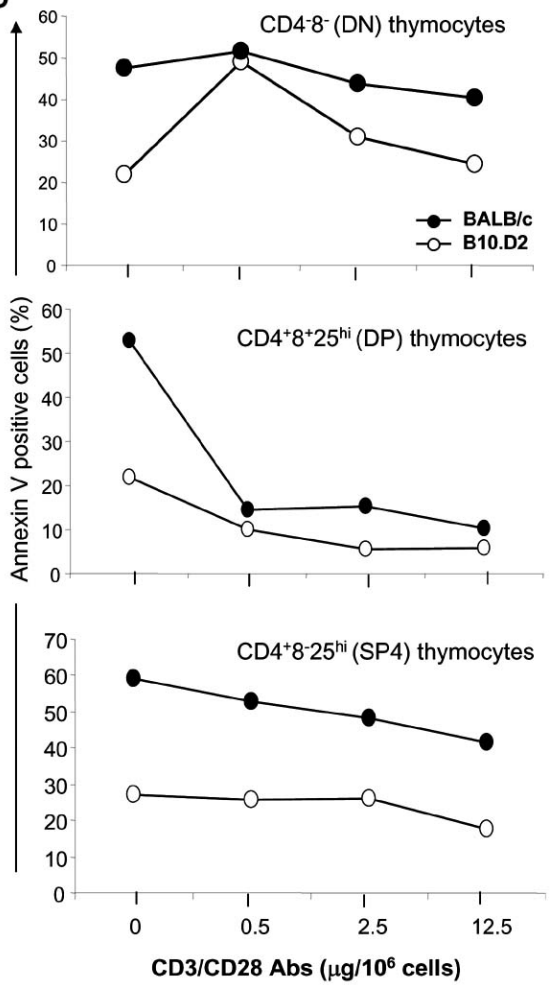

Fig. (6). ***In vitro*** **sensitivity of BALB/c and B10.D2 T-reg precursors to CD3-induced apoptosis.** (**A**) Thymocytes from BALB/c and B10.D2 mice (n = 5) were stained with CD4-FITC, CD8-PerCP, CD25-APC, and CD3ε-PE or CD28-PE Ab-conjugates, and analyzed for the CD3 and CD28 cell density by FACS. Shown are the MFI ± SD values of CD3 and CD28 receptors on DN, DP $CD25^{hi}$ and SP4 $CD25^{hi}$ T-reg precursors. (**B**) Thymocytes isolated from a pool of BALB/c and B10.D2 mice (n = 4) were stimulated for 24 h with various doses of soluble CD3ε and CD28 Abs, then washed and stained with CD4-FITC, CD8-PerCP, and CD25-APC Ab-conjugates and Annexin V-PE conjugate, and analyzed by FACS. Shown are the percent ± SD values of dying DN, DP $CD25^{hi}$ and SP4 $CD25^{hi}$ T-reg precursors in one of three representative experiments. Strength of CD3/CD28 stimulation (X-axis) refers to the amount of antibodies per 10^6 cells in 0.2 ml medium.

Variations in the T-Reg Thymic Output are Homeostatically Normalized in Periphery

The differential T-reg thymic output between the BALB/c and B10.D2 mice raised the question of whether the size of mature $CD4^+25^{hi}$ $Foxp3^+$ T-reg pool in the peripheral lymphoid organs is affected. While the frequency of terminally differentiated SP4 ($CD4^+8^-25^{hi}$ $Foxp3^+$) T-reg precursors was 3-times lower in BALB/c than in B10.D2 mice (1.54 ± 0.67% *vs*. 4.15 ±. 0.91%), the frequency of mature $CD4^+25^{hi}$ $Foxp3^+$ T-reg cells in the spleen of both strains was in a close range (6.8 ± 1.4% and 7.5 ± 1.2% respectively). Furthermore, the analysis of cell cycle divisions of splenic, mature $CD4^+25^{hi}$ $Foxp3^+$ T-regs from CSFE-labeled mice showed different proliferation rates *in vivo* in these strains. Splenic T-regs from both strains went to 4-5 cycles of homeostatic division within a 4-day interval, and to 7 cycles at the end of day 6 post-CFSE injection, but a significant number of splenic B10.D2 T-regs (32-35%) were slow-dividing (2-3 cycles of division within 6 days) (Fig. **7A**). Noteworthy, all mice investigated in this study were housed in a pathogen-free barrier, which rules out the possibility of opportunistic infections that may alter the T-cell homeostatic proliferation.

Since we found a strong correlation between the ObR partitioning on T-reg precursors and their rate of proliferation in BALB/c and B10.D2 mice, we next analyzed the ObR partitioning on splenic, mature $CD4^+25^{hi}$ $Foxp3^+$ T-reg cells. The patterns of ObR partitioning on splenic T-regs was similar to that on SP4 T-reg thymic precursors, since two major T-reg populations were detected, i.e., ObR^{lo} and ObR^{hi} T-regs (Fig. **7B**). However, in contrast to the pattern observed in the thymus, the B10.D2 mice showed a higher number of slow-dividing (ObR^{hi}) splenic T-regs than the BALB/c mice (53% *vs*. 33%). This was consistent with the CFSE results showing a larger population of slow-dividing splenic T-regs in B10.D2 mice than in BALB/c mice (Fig. **7A**). Furthermore, *in vitro* stimulation of splenic ObR^{hi} T-reg cells with leptin in the presence of CD3/CD28 Abs significantly inhibited the Cdk4 mRNA expression in both strains, indicating again that signaling of ObR leads to inhibition of T-reg proliferation (Fig. **7C**). This may well explain why the size of peripheral T-reg pool in B10.D2 mice having a higher T-reg thymic output was quiet similar to that of BALB/c mice having a lower T-reg thymic output. It thus appears that a switch in the ObR cell density occurs in periphery in the T-reg cells in these two strains that may compensate for the difference in their Foxp3 T-reg thymic output. This is consistent with previous reports showing that the requirements for T-reg clonal expansion in thymus are different than those in peripheral lymphopid organs [53].

Interesting enough, the overall ObR expression on ($CD25^{hi}$) T-reg thymic precursors was not only higher than that on conventional ($CD4^+25^-$) T-cell thymic precursors (Figs. **7B** *vs*. **7D**), but also showed a different pattern of partitioning. While the splenic T-reg cells showed two major populations (ObR^{lo} and ObR^{hi}), the conventional CD4 T-cells showed a predominant ObR^{lo} population.

Together, these results showed that the number of thymic T-reg immigrants does not affect significantly the size of peripheral T-reg compartment in these two mouse strains due to a homeostatic normalization. The ObR partitioning on T-reg cells appears to provide a negative signal for proliferation of T-reg precursors in thymus, and can also control their peripheral homeostasis. The cellular and molecular events leading to ObR re-partitioning in mature T-regs requires further investigations.

Differential T-Reg Development in BALB/C and B10.D2 Mice Echoes Their Suppressogenic Capacity in Periphery

Since a differential Foxp3 expression and $CD4^+25^{hi}$ T-reg thymic output did not affect the size of peripheral T-reg compartment in BALB/c and B10.D2 strains, we next investigated the function of mature, splenic T-reg cells in these strains. It has been suggested that the suppressogenic capacity of T-reg cells is much related to the amount of Foxp3 protein per cell. The *in vitro* suppressogenic capacity of splenic $CD4^+25^{hi}$ T-reg cells was tested using a transcriptomic approach relying on the mRNA expression level for Th1 and Th2 transcription factors in syngeneic $CD4^+25^-$ T helper responder cells in parallel with their ability to secrete cytokines upon CD3/CD28 stimulation. At the 1:1 ratio of T-regs to Th responders, the B10D2 T-regs inhibited almost 2-times stronger the IL-2 and IFN-γ secretion by Th responders than the BALB/c T-regs (Fig. **8A**, upper panel). Consistently, the Th1 and Th2 transcriptome expression (T-bet, STAT4, NFATc, STAT6, GATA3, and cMAF) was lower upon B10.D2 T-reg-induced suppression (Fig. **8A**, lower panel). These two assays indicated that the capacity of B10.D2 T-reg cells to suppress a Th response *in vitro* is stronger than that of BALB/c T-reg cells.

To compare the *in vivo* suppressogenicity of splenic $CD4^+25^{hi}$ T-reg cells from BALB/c and B10.D2 mice, we took advantage of an experimental autoimmune model for type 1 diabetes (T1D). In this system, RAG2 KO, RIP-HA Tg mice ($H\text{-}2^d$) expressing the influenza HA viral antigen in the pancreatic β-islets under the rat insulin promoter develop a rampant hyperglycemia (some 10-12 days) after infusion with diabetogenic (HA-specific) CD4 T-cells from mice bearing a TCR-$HA_{110\text{-}120}$ transgene (TCR-HA Tg T-cells/$H\text{-}2^d$) [10]. The suppressogenic capacity of splenic $CD4^+25^{hi}$ $Foxp3^+$ T-reg cells from BALB/c and B10.D2 mice was tested in relation to their ability to suppress the diabetogenic function of $CD4^+$TCR-HA T-cells *in vivo*. At the 1 to 2.5 ratio of T-regs to diabetogenic $CD4^+$ TCR-HA cells co-transferred in RAG2 KO RIP-HA mice, both the B10D.2 and BALB/c T-regs were unable to delay significantly the onset of hyperglycemia (Fig. **8B**, upper panel). However, only the B10.D2 T-regs prolonged the survival of hyperglycemic RAG2 KO, RIP-HA recipients (Fig. **8B**, lower panel). Some 80% of hyperglycemic recipients receiving B10D2 T-reg cells survived for 1 month after the onset of hyperglycemia. Prolonged survival occurred in the context of a protective peri-islet pancreatic infiltration with lymphocytes (Fig. **8C**). In contrast, only 50% of the hyperglycemic RAG2 KO, RIP-HA mice receiving BALB/c T-regs survived two weeks after hyperglycemia onset, and displayed a higher degree of destructive (intra-islet) β-islet infiltration. Thus, the number of heavily infiltrated β-islets in diabetic mice receiving B10.D2 T-regs (10 ±2 islets of 20 scored per pancreas in 3 individual mice) was lower than in those receiving BALB/c T-regs (16 ± 3 islets of 20 scored per pancreas in 3 individual mice).

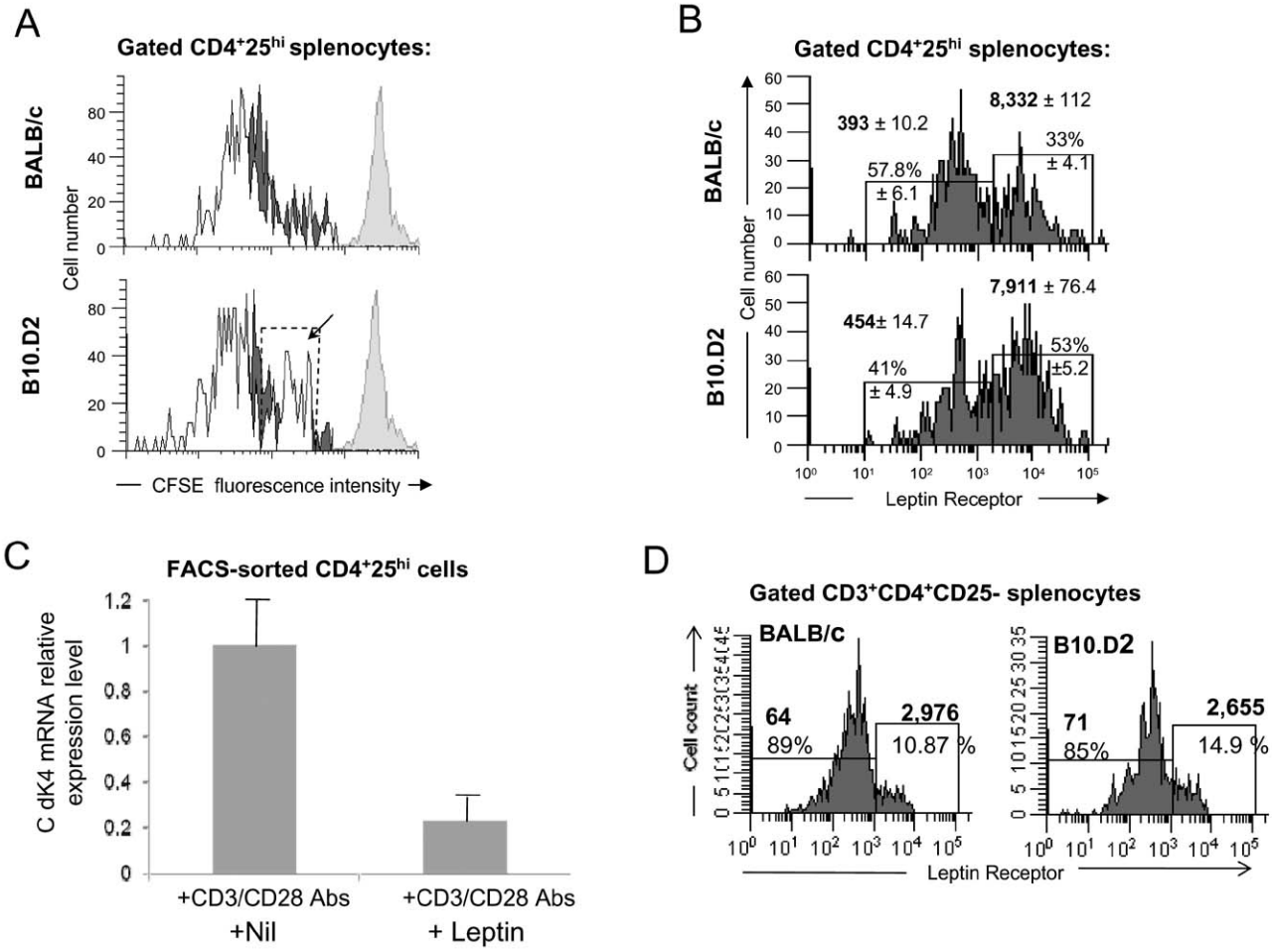

Fig. (7). Homeostatic normalization of splenic, mature CD4$^+$25^{hi} T-reg pool in BALB/c and B10.D2 mice. (**A**) Mice (n = 5) were injected i.v. with CFSE, and four and six days later the splenocytes were stained with CD4-PE-Cy7 and CD25-APC Ab-conjugates. The number of cell cycle divisions in FACS-gated CD4$^+$25^{hi} thymocytes was established based on the dilution factor for CFSE fluorescence The percent of proliferating T-reg cells in each cycle of division was determined using the ModFit analysis software. Shown is one of five representative mice in each group. Empty histograms represent day 6, and dark histograms represent day 4 post-CFSE injection. Arrow in the middle panel indicates the presence of a slow-dividing CD4$^+$25^{hi} T-reg population in the spleen of a B10.D2 mouse. Lower panel shows the CFSE fluorescence after five serial, twofold dilutions *in vitro* (empty plots) as compared with the uptake of CFSE by thymocytes *in vivo* at 30 min after CFSE injection (dark plot). (**B**) ObR partitioning on FACS-gated CD4$^+$25^{hi} T-reg splenic cells from BALB/c and B10.D2 mice as determined by FACS using ObR-FITC Ab-conjugate (BD PharMingen). Same mice used for thymic ObR measurements as described in figure 2 (panel b) were used in this experiment. Shown are the MFI ± SD values (bold), and percent of CD4$^+$CD25^{hi} splenocytes from individual mice (n = 4 per group) expressing low and high ObR density on the surface. (**C**) Effect of leptin on Cdk4 mRNA expression in splenic ObR^{hi} T-reg cells. FACS-sorted ObR^{hi}CD4$^+$CD25^{hi} splenocytes from BALB/c mice were stimulated for 24 h *in vitro* with CD3/CD28 Abs (5 μg/10^6 cells) in the presence or absence of mouse recombinant leptin (5 μg/10^6 cells), and the Cdk4 mRNA expression was measured by real-time RT-PCR. Shown are the mean +/- SD results for three individual mice. Similar results were obtained in ObR^{hi}CD4$^+$CD25^{hi} splenocytes from B10.D2 mice. (**D**) Partitioning of ObR on mature CD4 T-cells from the spleen of BALB/c and B10.D2 mice as determined by FACS using ObR-FITC Ab-conjugate (BD PharMingen). Shown are the MFI ± SD values (bold), and percent of ObR^{low} and ObR^{high} populations within the gated CD3$^+$CD4$^+$CD25$^-$ splenocytes from a pool of five mice in each group.

The autoimmune diabetes system demonstrated that the B10.D2 T-regs provides a stronger protection against pancreatic infiltration than their BALB/c counterparts. The explanation for a higher suppressogenic capacity of splenic B10.D2 T-regs may well account for their higher Foxp3 protein expression as determined by single-cell level FACS (Fig, **8D**), and 1.5-2-times higher level of Foxp3 mRNA measured by real-time RT-PCR.

Together, these results indicated that a differential T-reg thymic development in mice with different genetic background does not affect the size of peripheral CD4$^+$25^{hi} Foxp3$^+$ T-reg pool due to a homeostatic normalization, but it does affect their suppressogenic function.

DISCUSSION

Foxp3 incited much interest as the master regulatory gene of thymic development and suppressogenic function of

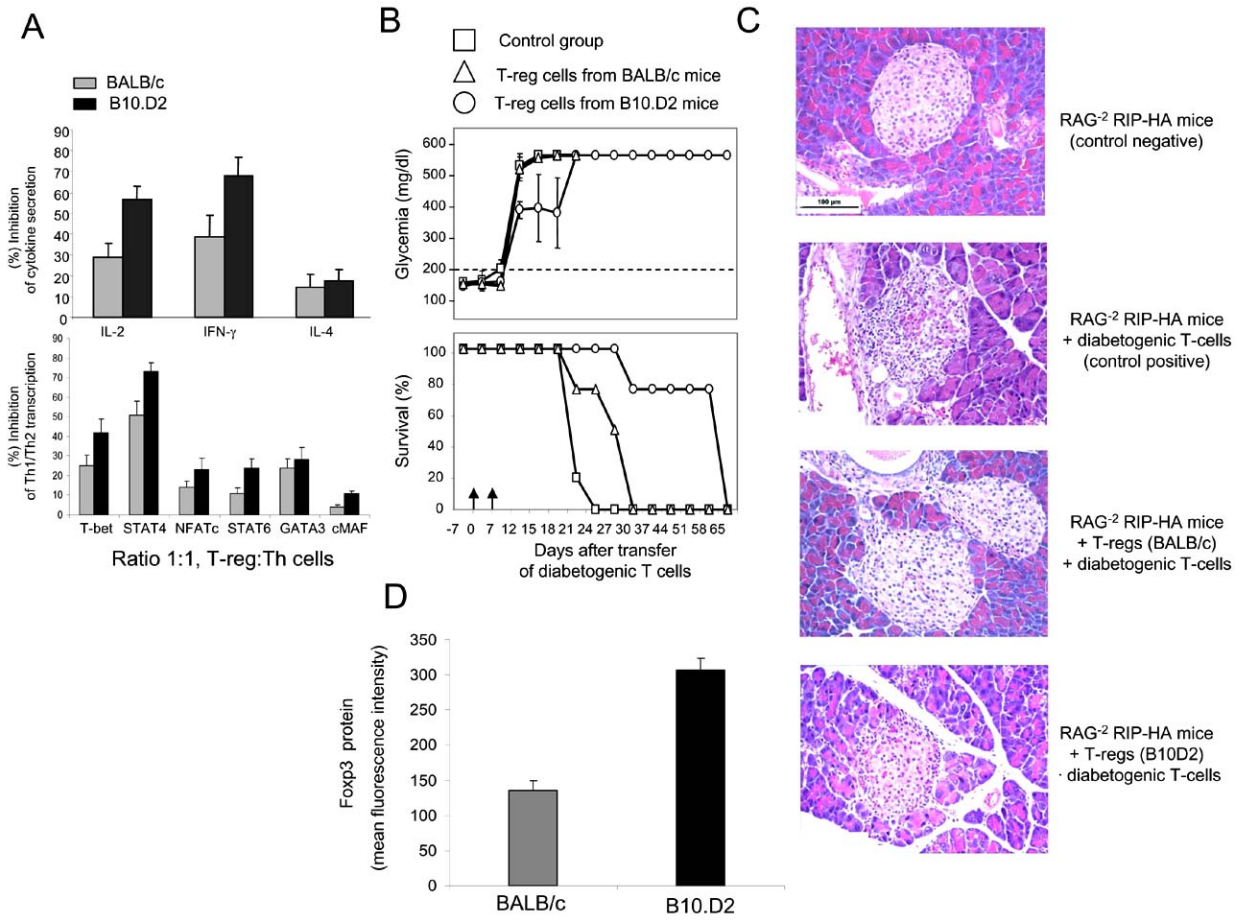

Fig. (8). Suppressogenicity of splenic, mature T-regs from BALB/c and B10.D2 mice. (**A**) *In vitro* suppression assay. The $CD4^+25^-$ T cell responders ($5x10^5$ cells) from the spleens of BALB/c or B10.D2 mice (pool of 5 mice per group) were isolated on CD4 mouse columns followed by CD25 immunobeads, and then co-incubated for 24 h on CD3 and CD28 Ab stimulation (2.5 μg/$5x10^5$ cells) with FACS-sorted, syngeneic $CD4^+25^{hi}$ T-reg cells ($5x10^5$ cells). From the same culture wells, the supernatants were assessed for cytokine secretion by ELISA, and the cell pellets were assessed for the mRNA expression level of Th1 and Th2 transcriptional factors by real-time PCR. Shown is the mean inhibition ±SD of IL-2, IL-4, and IFN-γ from two identical experiments in which the signal-to-noise signal generated in the T responders/T-reg co-culture in the absence of CD3 and CD28 stimulation were subtracted (*upper panel*). The percent inhibition of cytokine secretion (Y-axis) was determined in relation to the corresponding amount of IL-2, IL-4 and IFN-γ (pg/ml) secreted by $CD4^+25^-$ T cell responders stimulated with CD3/CD28 Abs in the absence of T-reg cells. The quantitative measurements of mRNA relative expression for T-bet, STAT4, NFATc, STAT6, GATA3, and cMAF were carried out by real-time PCR (*lower panel*) (specific primers, Applied Biosystems, Foster City, CA). The percent inhibition for each transcription factor (Y-axis) was calculated as percent of mRNA obtained by real-time PCR from $CD4^+25^-$ T cell responders stimulated with CD3/CD28 Abs in the absence of T-reg cells. (**B**) *In vivo* suppression assay. RAG2 KO, RIP-HA Tg mice infused with splenic T-reg cells (10^5 cells from a pool of five BALB/c or five B10.D2 mice) (arrow at day 0 on X-axis), and 7 days later infused with diabetogenic, splenic T cells ($2.5x10^5$ cells from a pool of five TCR-HA Tg mice) (arrow at day 7 on X-axis). Shown are the glycemia values (*upper panel)* and the percent survival (*lower panel)* of RAG2 KO, RIP-HA Tg recipients. The dotted line (*upper panel*) indicates the upper limit of normoglycemia previously determined in a cohort of twelve non-infused (control) RAG2 KO, RIP-HA Tg mice. (**C**) Hematoxilin-eosin staining of 0.5 μ pancreatic cross-sections from RAG2 KO, RIP-HA Tg recipients treated as in panel B, at 1 week after infusion of diabetogenic T-cells. Shown is one of twenty representative pancreatic islets from each group of mice. (**D**) Quantification of Foxp3 protein at the single-cell level in BALB/c and B10.D2 splenic T-reg cells was carried out based on the mean fluorescence intensity (MFI) in $CD4^+CD25^{hi}$ splenocytes intra-nuclearly stained with Foxp3 APC-Ab conjugate. Shown are the MFI mean ±SD values in groups of six mice.

$CD4^+25^{hi}$ T-reg cells. Foxp3 transcripts were recently detected in the early DN0 ($CD3^-4^-8^-$) stage of thymic differentiation in humans [54]. Herein, we detected Foxp3 mRNA and Foxp3 protein early during the DN3/4 stages of thymic differentiation in two different genetic backgrounds (BALB/c and B10.D2 mice) sharing the same MHC class II ($H\text{-}2^d$) haplotype. Foxp3 was differentially expressed in BALB/c and B10.D2 T-reg precursors through all stages of thymic differentiation. An epigenetic control of Foxp3 gene was suggested based on the polymorphism in the Foxp3 binding sites for transcription factors like ATF/CREB, C/EBP-γ, Elk-1, Ets-1, GATA-4, NFATc, NF-kB, SMAD-4, STAT-1, TGF-4, and TTF1 [51]. Inasmuch as DNA methylation events assist the chromatin-remodeling and the circadian

clock-regulated gene expression during differentiation of T-cells toward a Th1 or Th2 phenotype [47, 55], similar events may play a role in T-reg thymic differentiation. Our DNA methylation assay ruled out the possibility that epigenetic alterations such as methylation in the Foxp3 gene promoter in T-reg precursors could be the mechanism responsible for variations in thymic expression of Foxp3 gene in BALB/c and B10.D2 mice. However, DNA methylation in the 1st *Foxp3* intron was recently described to be inversely correlated with the binding of CREB/ATF complex transcription factor and Foxp3 expression [56], and further investigations are required to find out whether a polymorphism in Foxp3 non-coding regions may lead to variations in Foxp3 expression in different genetic backgrounds. Epigenetic alterations may affect not only the Foxp3 *locus*, but also *loc*i encoding modulators of cell cycle division and apoptosis in T-reg precursors, as suggested by our experiments revealing a differential expression of Bad, Caspase 3, ObR, and CD3 in T-reg precursors from BALB/c and B10.D2 mice. More than 700 genes have been recently identified to be up- and down-regulated in developing and mature $CD4^+25^{hi}$ T-reg cells from C57BL/6 mice, and several polymorphic genes with unique expression in different genetic backgrounds were also found to affect the thymic differentiation of T-reg cells [57].

The Foxp3 thymic output was almost 3-times higher in B10.D2 mice than in BALB/c mice. A differential $CD4^+25^{hi}$ thymic output between the B6, DBA/2 and SJL inbred mice bearing different MHC class II haplotypes was previously described [58]. Herein, we found a dual mechanism associated with the differential T-reg thymic output in BALB/c and B10.D2 mice. One arm of this mechanism appears to control the rate of T-reg thymic proliferation. Higher rates of proliferation were associated with a larger number of fast-dividing (ObR^{lo}) $Foxp3^+$ thymocytes. In addition, besides the negative signaling of T-reg proliferation through ObR, its high cell density on T-reg precursors and mature $CD4^+25^{hi}$ T-reg cells as compared with conventional T-cells suggests that ObR is a new biomarker for T-regs.

A second regulatory event that contributed to a differential T-reg thymic output in BALB/c and B10.D2 mice was apoptosis of T-reg precursors. Higher rates of T-reg apoptosis in BALB/c mice than in B10D2 mice occurred in the context of an increased basal level of Bad and Caspase 3 expression. Thus, the DN3/4 transition stage of thymic differentiation appeared to be not only the earliest time-point of Foxp3 expression in T-reg precursors, but also the earliest checkpoint for T-reg negative selection. Indeed, the thymic cortical area where most of the DN thymocytes reside displays a high extend of cell death [59]. Not surprisingly, the DN thymocytes can receive CD3/TCR signals in the absence of a CD4 receptor, since the $p56^{lck}$ phosphorylation and segregation of pre-TCRα in the plasma membrane lipid rafts occurs in DN thymocytes as well [60]. Furthermore, we found that a lower CD3, but not CD28 cell density on B10.D2 T-reg precursors than on their BALB/c counterparts was associated with a lower sensitivity to CD3-induced apoptosis in the DN and DP stages of thymic differentiation. In contrast, the T-reg precursors showed similar CD3 cell density in the SP4 terminal stage of thymic differentiation in both mouse strains, and their sensitivity to CD3-induced apoptosis was negatively correlated with the strength of CD3 signaling. Stronger CD3 stimulation provided better protection against apoptosis. It thus appears that CD3, but not CD28 stimulation plays an important role in thymic selection of T-reg cells.

Interesting enough, a differential T-reg thymic output between the BALB/c and B10.D2 mice did not affect the size of splenic $CD4^+25^{hi}$ T-reg pool due to a regulatory homeostatic mechanism. Previous data showed that the T-reg thymic output in various mouse strains lacks correlation with the size of T-reg compartment in periphery [58]. The T-reg homeostatic proliferation in the spleen of BALB/c mice was more accelerated than in B10.D2 mice, and this occurred in the context of a larger number of fast-dividing (ObR^{lo}) T-reg cells than in B10.D2 mice. However, the T-reg suppressogenic capacity was different in these two strains, since the splenic T-regs from B10.D2 mice were more suppressogenic in the context of a higher expression of Foxp3 protein per cell.

CONCLUSION REMARKS

In summary, this study revealed a differential tuning of key regulatory proteins for thymic proliferation and apoptosis of $CD4^+Foxp3^+$ T-reg cells that appear to be under the genetic control unrelated to the MHC class II genes. This was associated with variations in the T-reg thymic output in two different mouse strains. A dual mechanism responsible for differential rates of proliferation and apoptosis in T-reg precursors in two different mouse strains seemed to rely on the cell density of several receptors and signaling molecules such as the leptin receptor (ObR), CD3/TCR complex, Bad, and Caspase 3. The differential T-reg thymic output was homeostatically normalized in periphery, whereas their suppressogenic capacity was not. A stronger suppressogenic capacity of peripheral, mature T-reg cells was paralleled by a higher Foxp3 expression per cell. The differential thymic development and function of $CD4^+Foxp3^+$ T-reg cells in different genetic backgrounds may explain at least in part the variations in susceptibility to infections and autoimmune disorders reported in individuals from different ethnic groups. Recently, correlates between the genetic polymorphism at (GT)n, (TC)n1, DXS573, and DXS120B loci in Foxp3 gene, and variations in susceptibility to autoimmune thyroiditis between Caucasian and Japanese ethnic groups, have been reported [61].

ACKNOWLEDGEMENTS

This work was supported by grants from the National Institutes of Health, DK61927 & DK61326 to T-D.B. and DK077521 to S.C, and from JDRF-12002-1151 to SC and T-D.B. We thank Mrs. Karen Wolcott and Kateryna Lund for technical assistance with FACS-sorting. The authors declare no competing financial conflict of interest.

REFERENCES

[1] Shevach EM. Regulatory T cells in autoimmunity. Ann Rev Immunol 2000; 18: 423-49.

[2] Takahashi T, Kuniyasu Y, Toda M, *et al*. Immunologic self tolerance maintained by $CD25^+CD4^+$ naturally anergic and suppressive T cells: induction of autoimmune disease by breaking their anergic/suppressive state. Int Immunol 1998; 10: 1969-80.

[3] von Herrath MG, Harrison LC. Antigen-induced regulatory T cells in autoimmunity. Nat Rev Immunol 2003; 3: 223-32.

[4] Groux H. An overview of regulatory T cells. Microbes Infect 2001; 3: 883-9.

[5] von Boehmer H. Mechanisms of suppression by suppressor T cells. Nat Immunol 2005; 6: 338-44.

[6] Hsu WT, Suen JL, Chiang BL. The role of CD4CD25 T cells in autoantibody production in murine lupus. Clin Exp Immunol 2006; 145: 513-9.

[7] Marrie RA, Jahlas SD, Bray GM. Familial autoimmune myastenia gravis: four patients involving three generations. Can J Neurol Sci 2000; 27: 307-10.

[8] Seddon B, Mason D. Regulatory T cells in the control of autoimmunity: the essential role of transforming growth factor beta and interleukin 4 in the prevention of autoimmune thyroiditis in rats by peripheral CD4+CD45RC- cells and CD4+CD8- thymocytes. J Exp Med 1999; 189: 279-88.

[9] Sanchez-Ramon S, Navarro AJ, Aristimuno C, *et al*. Pregnancy-induced expansion of regulatory T-lymphocytes may mediate protection to multiple sclerosis activity. Immunol Lett 2005; 96: 195-201.

[10] Casares S, Hurtado A, McEvoy RC, Sarukhan A, von Boehmer H, Brumeanu TD. Down-regulation of diabetogenic CD4+ T cells by a soluble dimeric peptide-MHC class II chimera. Nat Immunol 2002; 3: 383-91.

[11] Han HS, Jun HS, Utsugi T, Yoon JW. A new type of CD4+ T cells completely prevents spontaneous autoimmune diabetes ands recurrent diabetes in syngeneic islet-transplanted NOD mice. J Autoimmun 1996; 9: 331-9.

[12] Powrie F, Carlino J, Leach MW, Mauze S, Coffman RL. A critical role for transforming growth factor-beta but not interleukin 4 in the suppression of T helper type 1-mediated colitis by CD45RB(low) CD4 T cells. J Exp Med 1996; 183: 2669-74.

[13] Sakaguchi S, Sakaguchi N, Asano M, Itoh M, Toda M. Immunologic self tolerance maintained by T cells expressing IL-2 receptor alpha chains (CD25). Breakdown of a single mechanism of self tolerance causes various autoimmune diseases. J Immunol 1995; 155: 1151-64.

[14] Papiernik M, Banz A. Natural regulatory CD4 T cells expressing CD25. Microbes Infect 2001; 3: 937-45.

[15] Furtado GC, de Lafaille MA, Kutchukidze N, Lafaille JJ. Interleukin-2 signaling is required for $CD4^+$ regulatory T-cell function. J Exp Med 2002; 196: 851-7.

[16] Bayer AL, Yu A, Malek TR. Function of the IL-2R for thymic and peripheral CD4+CD25+ Foxp3+ T regulatory cells. J Immunol 2007; 178: 4062-71.

[17] Fontenot JD, Rasmussen JP, Gavin MA, Rudensky AY. A function for interleukin-2 in Foxp3 expressing regulatory T cells. Nat Immunol 2005; 6: 1142-51.

[18] Caramalho I, Carvalho TL, Ostler D, Zelenay S, Haury M, Demengeot J. Regulatory T cells selectively express toll-like receptors and are activated by lipopolysaccharide. J Exp Med 2003; 197: 403-11.

[19] McHugh RS, Whitters MJ, Piccirillo CA, Young DA, Sevach EM, Byrne MC. CD4+CD25+ immunoregulatory T cells: gene expression analysis reveals a functional role for the glucocorticoid-induced TNF receptor. Immunity 2002; 16: 311-23.

[20] Kubach J, Lutter P, Bopp T, *et al*. Human CD4+CD25+ regulatory T cells: proteome analysis identifies galectin-10 as a novel marker essential for their anergy and suppressive function. Blood 2007; 110: 1550-8.

[21] De Rosa V, Procaccini C, Cali G, *et al*. A key role of leptin in the control of regulatory T cell proliferation. Immunity 2007; 26: 241-55.

[22] Read S, Greenwald R, Izcue A, *et al*. Blockade of CTLA-4 on CD4+25+ regulatory T cells abrogates their function *in vivo*. J Immunol 2006; 177: 4376-83.

[23] Hori S, Nomura T, Sakaguchi S. Control of regulatory T cell development by the transcription factor Foxp3. Science 2003; 299: 1057-61.

[24] Fontenot JD, Rasmussen JP, Williams LM, Dooley JL, Farr AG, Rudensky AY. Regulatory T cell lineage specification by the forkhead transcription factor foxp3. Immunity 2005; 22: 329-41.

[25] Campbell DJ, Ziegler SF. FOXP3 modifies the phenotypic and functional properties of regulatory T cells. Nat Rev Immunol 2007; 7: 305-10.

[26] Wildin RS, Smyk-Pearson S, Filipovich AH. Clinical and molecular features of the immunodysregulation, polyendocrinopathy, enteropathy, X linked (IPEX) syndrome. J Med Genet 2002; 39: 537-45.

[27] Boyer O, Saadoun D, Abriol J, Dodille M, Piette JC, Cacoub P, Klatzmann D. $CD4^+CD25^+$ regulatory T-cell deficiency in patients with hepatitis C-mixed cryoglobulinemia vasculitis. Blood 2004; 103: 3428-30.

[28] Longhi MS, Ma Y, Bogdanos DP, Cheeseman P, Mieli-Vergani G, Vergani D. Impairment of $CD4^+CD25^+$ regulatory T-cells in autoimmune liver disease. J Hepatol 2004; 41: 31-7.

[29] de Kleer IM, Wedderburn LR, Taams LS, *et al*. $CD4^+$CD25 bright regulatory T cells actively regulate inflammation in the joints of patients with the remitting form of juvenile idiopathic arthritis. J Immunol 2004; 172: 6435-43.

[30] Cao D, van Vollenhoven R, Klareskog L, Trollmo C, Malmström V. CD25 bright $CD4^+$ regulatory T cells are enriched in inflamed joints of patients with chronic rheumatic disease. Arthritis Res Ther 2004; 6: R335-46.

[31] Crispin JC, Martínez A, Alcocer-Varela J. Quantification of regulatory T cells in patients with systemic lupus erythematosus. J Autoimmun 2003; 21: 273-6.

[32] Furuno K, Yuge T, Kusuhara K, *et al*. $CD25^+CD4^+$ regulatory T cells in patients with Kawasaki disease. J Pediatr 2004; 145: 385-90.

[33] Viglietta V, Baecher-Allan C, Weiner HL, Hafler DA. Loss of functional suppression by $CD4^+CD25^+$ regulatory T cells in patients with multiple sclerosis. J Exp Med 2004; 199: 971-9.

[34] Putheti P, Pettersson A, Soderstrom M, Link H, Huang YM. Circulating $CD4^+CD25^+$ T regulatory cells are not altered in multiple sclerosis and unaffected by disease-modulating drugs. J Clin Immunol 2004; 24: 155-61.

[35] Lindley S, Dayan CM, Bishop A, Roep BO, Peakman M, Tree TI. Defective suppressor function in $CD4^+CD25^+$ T-cells from patients with type 1 diabetes. Diabetes 2005; 54: 92-9.

[36] Putnam AL, Vendrame F, Dotta F, Gottlieb PA. $CD4^+$CD25 high regulatory T cells in human autoimmune diabetes. J Autoimmun 2005; 24: 55-62.

[37] Gottenberg JE, Lavie F, Abbed K, *et al*. CD4 CD25 high regulatory T cells are not impaired in patients with primary Sjögren's syndrome. J Autoimmun 2005; 24: 235-42.

[38] Balandina A, Lécart S, Dartevelle P, Saoudi A, Berrih-Aknin S. Functional defect of regulatory $CD4^+CD25^+$ T cells in the thymus of patients with autoimmune myasthenia gravis. Blood 2005; 105: 735-41.

[39] Fattorossi A, Battaglia A, Buzzonetti A, Ciaraffa F, Scambia G, Evoli A. Circulating and thymic $CD4^+CD25^+$ T regulatory cells in myasthenia gravis: effect of immunosuppressive treatment. Immunology 2005; 116: 134-41.

[40] Ehrenstein MR, Evans JG, Singh A, *et al*. Compromised function of regulatory T cells in rheumatoid arthritis and reversal by anti-TNFalpha therapy. J Exp Med 2004; 200: 277-85.

[41] Möttönen M, Heikkinen J, Mustonen L, Isomäki P, Luukkainen R, Lassila O. $CD4^+$ $CD25^+$ T cells with the phenotypic and functional characteristics of regulatory T cells are enriched in the synovial fluid of patients with rheumatoid arthritis. Clin Exp Immunol 2005; 140: 360-7.

[42] Vigna-Pérez M, Abud-Mendoza C, Portillo-Salazar H, *et al*. Immune effects of therapy with Adalimumab in patients with rheumatoid arthritis. Clin Exp Immunol 2005; 141: 372-80.

[43] Thomas S, Preda-Pais A, Kumar RS, Casares S, Brumeanu T-D. A model for antigen-specific T-cell anergy: displacement of CD4-p56lck signalosome from the lipid rafts by a soluble, dimeric peptide-MHC II chimera. J Immunol 2003; 170: 5981-92.

[44] Fleck M, Zhou T, Tatsuta T, Yang P, Wang Z, Mountz JD. Fas/Fas ligand signaling during gestational T cell development. J Immunol 1998; 160: 3766-75.

[45] Cefai D, Favre L, Wattendorf E, Marti A, Jaggi R, Gimmi CD. Role of FAS ligand expression in promoting escape from immune rejection in a spontaneous tumor model. Int J Cancer 2001; 91: 529-37.

[46] Weber S, Traunecker A, Oliveri F, Gerhard W, Karjalainen K. Specific low-affinity recognition of major histocompatibility complex plus peptide by soluble T-cell receptor. Nature 1992; 356: 793-6.

[47] Guo L, Hu-Li J, Paul WE. Probabilistic regulation of IL-4 production in Th2 cells: accessibility at the IL-4 locus. Immunity 2004; 20: 193-203.

[48] Lind EF, Prockop SE, Porritt HE, Petrie HT. Mapping precursor movement through the postnatal thymus reveals specific microen-

vironments supporting defined stages of early lymphoid development. J Exp Med 2001; 194: 127-34.
[49] Starr TK, Jameson SC, Hogquist KA. Positive and negative selection of T cells. Annu Rev Immunol 2003; 21: 139-76.
[50] Maggi E, Cosmi L, Liotta F, Romagnani P, Romagnani S, Annunziato F. Thymic regulatory T cells. Autoimmun Rev 2005; 4: 579-86.
[51] Floess S, Freyer J, Siewert C, *et al*. Epigenetic control of the Foxp3 locus in regulatory T cells. PLos Biol 2007; 5: 169-78.
[52] Brumeanu T-D, Preda-Pais A, Stoica C, Bona C, Casares S. Differential partitioning and trafficking of GM gangliosides and cholesterol-rich lipid rafts in thymic and splenic CD4 T cells. Mol Immunol 2007; 44: 530-40.
[53] Apostolou I, Sarukhan A, Klein L, von Boehmer H. Origin of regulatory T cells with known specificity for antigen. Nat Immunol 2002; 3: 756-63.
[54] Tuovinen H, Kekalainen E, Rossi LH, Puntila J, Arstila PT. Human CD4-CD8- thymocytes express FOXP3 in the absence of a TCR. J Immunol 2008; 180: 3651-4.
[55] Winders BR, Schwartz RH, Bruniquel D. A distinct region of the murine IFN-gamma promoter is hypomethylated from early T cell development through mature naive and Th1 cell differentiation, but is hypermethylated in Th2 cells. J Immunol 2004; 173: 7377-84.
[56] Kim HP, Leonard WJ. CREB/ATF-dependent T cell receptor-induced FoxP3 gene expression: a role for DNA methylation. J Exp Med 2007; 204: 1543-51.
[57] Zheng Y, Josefowicz SZ, Kas A, Chu T-T, Gavin MA, Rudensky AY. Genome-wide analysis of Foxp3 target genes in developing and mature regulatory T cells. Nature 2007; 445: 936-40.
[58] Romagnoli P, Tellier J, van Meerwijk JPM. Genetic control of thymic development of CD4+CD25+Foxp3+ regulatory T lymphocytes. Eur J Immunol 2005; 35: 3525-32.
[59] Surh CD, Sprent J. T-cell apoptosis detected in situ during positive and negative selection in the thymus. Nature 1994; 372: 100-3.
[60] Saint-Ruf C, Panigada M, Azogui O, Debey P, von Boehmer H, Grassi F. Different initiation of pre-TCR and gamma delta TCR signaling. Nature 2000; 406: 524-7.
[61] Ban Y, Tozaki T, Tobe T, *et al*. The regulatory T cell gene FOXP3 and genetic susceptibility to thyroid autoimmunity: An association analysis in Caucasian and Japanese cohorts. J Autoimmun 2007; 28: 201-7.

Received: March 09, 2009 Revised: June 09, 2009 Accepted: June 12, 2009